Available online at www.sciencedirect.com
SCIENCE DIRECT®
Journal of Catalysis 242 (2006) 1–15
JOURNAL OF CATALYSIS
www.elsevier.com/locate/jcat

First-principles-based kinetic Monte Carlo simulation of the selective hydrogenation of acetylene over Pd(111)

Donghai Mei [a], Priyam A. Sheth [a], Matthew Neurock [a,b,*], C. Michael Smith [c]

[a] *Department of Chemical Engineering, University of Virginia, Charlottesville, VA 22904, USA*
[b] *Department of Chemistry, University of Virginia, Charlottesville, VA 22904, USA*
[c] *The Dow Chemical Company, Freeport, TX 77541-3257, USA*

Received 24 January 2006; revised 30 April 2006; accepted 2 May 2006

Available online 23 June 2006

Abstract

The kinetics for the selective hydrogenation of acetylene over Pd(111) was investigated by using first-principles-based kinetic Monte Carlo simulations. Density functional theory (DFT) calculations were carried out to obtain intrinsic kinetic data for a Horiuti–Polanyi-type reaction mechanism involving the sequential hydrogenation of acetylene. The results were subsequently used to develop a detailed intrinsic kinetics database that includes the adsorption energies of the reactants, intermediates, and products, the reaction energies and activation barriers of the elementary steps in the proposed reaction mechanism. The DFT-calculated energies and activation barriers were initially performed at lower surface coverages, to probe the intrinsic surface chemistry. Subsequent calculations were carried out at higher coverages, to capture the influence of the local environment on the reaction kinetics, and used to parameterize coarse-grained models that describe adsorbate interactions. A van der Waals force field model and a modified bond order conservation model were subsequently used within the simulation to calculate the local *through-space* interactions and the lateral *through-surface* interactions occurring between coadsorbates, respectively, and to assess the influence of the local reaction environment. The intrinsic DFT-derived kinetic data and the coarse-grained reaction environment models were used together in a variable time step kinetic Monte Carlo simulation to track the molecular transformations involved in acetylene hydrogenation over the (111) surface of Pd. The kinetic Monte Carlo simulation method [E.W. Hansen, M. Neurock, Chem. Eng. Sci. 54 (1999) 3411; E.W. Hansen, M. Neurock, J. Catal. 196 (2000) 241; E.W. Hansen, M. Neurock, Surf. Sci. 464 (2000) 91; E.W. Hansen, M. Neurock, J. Phys. Chem. B 105 (2001) 9218] used herein explicitly treats the atomic surface structure, the effects of the local reaction environment, and the reaction conditions on the surface kinetics. The simulated apparent activation energy for acetylene hydrogenation was calculated as 8.0 ± 0.6 kcal/mol at $P_{H_2} = 100$ Torr and $P_{C_2H_2} = 100$ Torr over the temperature range of 300–500 K, in very good agreement with the value of 9.6 kcal/mol reported from experimental studies over well-defined Pd(111) surfaces [H. Molero, B.F. Bartlett, W.T. Tysoe, J. Catal. 181 (1999) 49]. The reaction orders were calculated as -0.52 ± 0.03 for acetylene and 1.16 ± 0.03 for hydrogen, which agree very well with the experimental reaction orders by Molero et al. [H. Molero, B.F. Bartlett, W.T. Tysoe, J. Catal. 181 (1999) 49] of -0.66 and 1.04, respectively. A comparison of the simulations carried out assuming non-interacting adsorbates (hard sphere) and those that include lateral interactions between adsorbates showed that although the overall apparent activation energy was weakly sensitive to the presence of lateral interactions, the surface coverages and intrinsic rates changed considerably due to the presence of lateral interactions. The addition of lateral interactions between coadsorbates was found to be essential in simulating the correct overall selectivity behavior and appropriately predicting the apparent reaction orders with respect to hydrogen and acetylene.

Keywords: Acetylene hydrogenation; Palladium; DFT; Kinetic Monte Carlo simulation; Ab initio quantum chemical; Ethylene hydrogenation; Pd(111); Lateral interactions

1. Introduction

The catalysts used in the polymerization of ethylene to polyethylene are quite sensitive to the amount of acetylene, which is typically within the range of 0.5–2 vol% in refined ethylene feedstocks [6–10]. These feedstocks must first be hydrogenated

* Corresponding author.
E-mail address: mn4n@virginia.edu (M. Neurock).

0021-9517/$ – see front matter
doi:10.1016/j.jcat.2006.05.009

$$2\{H_2(g) + 2^* \leftrightarrows H^* + H^*\} \quad (1)$$

$$HC{\equiv}CH(g) + {}^* \leftrightarrows HC{\equiv}CH^* \quad (2)$$

$$HC{\equiv}CH^* + H^* \leftrightarrows H_2C{=}CH^* + {}^* \quad (3)$$

$$H_2C{=}CH^* + H^* \leftrightarrows H_2C{=}CH_2^* + {}^* \quad (4)$$

$$H_2C{=}CH_2^* \leftrightarrows H_2C{=}CH_2(g) + {}^* \quad (5)$$

$$H_2C{=}CH_2^* + H^* \leftrightarrows H_3C{-}CH_2^* + {}^* \quad (6)$$

$$H_3C{-}CH_2^* + H^* \leftrightarrows H_3C{-}CH_3^* + {}^* \quad (7)$$

$$H_3C{-}CH_3^* \leftrightarrows H_3C{-}CH_3(g) + {}^* \quad (8)$$

Scheme 1. Hydrogen addition reactions, where * denotes one empty surface site and the species identified with * denote an adsorbed intermediate.

to reduce the acetylene impurities to <5 ppm, to prevent the deactivation of olefin polymerization catalysts. The hydrogenation of acetylene from ethylene feeds is generally carried out in a fixed-bed reactor over supported Pd catalysts in two different types of processes known as front-end and tail-end processes [6,10,11], with the terms referring to the location of the hydrogenation reactor within the overall ethylene plant. In the front-end process, acetylene hydrogenation is carried out just before the methanation unit, whereby the feed contains acetylene together with fair amounts of hydrogen and light hydrocarbons. The partial pressure of hydrogen in the front-end process is typically much greater than that in the tail-end process. The higher pressures of hydrogen increase the rate of acetylene hydrogenation and limit the formation of carbon deposits. In the tail-end process, acetylene hydrogenation is carried out after the de-ethanizer unit, where the feed is typically ethylene rich [6,10,11]. Tail-end acetylene processes are typically run at significantly lower partial pressures of hydrogen, at which reactor runaway is not an issue. The lower partial pressures of hydrogen, however, can lead to the development of carbonaceous deposits and the formation of green oil, which can cover the catalyst and significantly lower the reaction rate [12].

It is now generally accepted that acetylene hydrogenation over Pd follows a sequential series of hydrogen addition reactions [13–17], such as those shown in Scheme 1. This is the classical Horiuti–Polanyi mechanism [18], which involves the sequential hydrogenation of acetylene and its subsequent hydrocarbon intermediates, thus resulting in the desired ethylene and undesired ethane products. These reactions tend to follow Langmuir–Hinshelwood rather than Eley–Rideal paths [13–16, 19].

The selective hydrogenation of acetylene reaction is typically carried out over supported Pd particles and is fairly selective, thus actively catalyzing acetylene hydrogenation while minimizing ethylene hydrogenation. The selectivity to acetylene hydrogenation was initially proposed to be the result of thermodynamic adsorption differences between acetylene and ethylene [20]. More recent explanations, however, suggest that mechanistic differences may control the differences in hydrogenation activities between acetylene and ethylene. These explanations are more consistent with the experimental observations that accompany ethylene hydrogenation as well as carbonaceous product formation [21–25]. They point to the differences in the relative reaction rates of the elementary steps as being responsible for the overall selectivity of acetylene hydrogenation to ethylene. Therefore, the selectivity for acetylene hydrogenation depends not only on the surface coverage of the reaction intermediates, but also on the local reaction environment surrounding the active intermediates. In the case of acetylene, for example, acetylene will not form a well-defined overlayer when adsorbed at temperatures over 200 K in the presence of hydrogen [26]. This is thought to be due to changes in the sticking probability of acetylene in the presence of hydrogen. Furthermore, on heating, acetylene decomposes into ethylidyne, as seen by LEED [27]. Ethylidyne can subsequently decompose into carbonaceous deposits on further heating, as reported by Tysoe [28] and Kesmodel [29]. These observations on acetylene indicate that selectivity is controlled by the elementary steps involving the adsorption of acetylene as well as its different reaction paths. In addition, certain sequences of coupling pathways can lead to the formation of C_4 intermediates that can subsequently go on to form oligomers, which can deactivate the catalyst. *Mechanistic effects* appear to be important in determining the selectivity in acetylene hydrogenation. Mechanistic effects were also seen to be important in our earlier theoretical results [30,31] that specifically examined the relative rates for acetylene and ethylene hydrogenation. These studies indicated that vinyl was a key surface intermediate, because different surface intermediates can form from vinyl depending on the reaction environment around the vinyl species. Thus these studies strongly suggest that all of these reaction paths need to be included in the development of a detailed reaction mechanism and a rate model for the catalytic selective hydrogenation of acetylene.

Many of the analytical reaction rate models for acetylene hydrogenation developed over the past 30 years were reviewed by Bos and Westerterp [12,32], who compared the validity of these models under different experimental conditions. Nearly all of the models predict the reaction order for hydrogen to be between 1.0 and 1.5 and that for acetylene to be between 0.0 and −0.5 with respect to the overall rate of acetylene hydrogenation. But the rate constants used for the different rate models are typically only applicable at the reaction conditions under which they were regressed. The local surface coverage for different intermediates is typically ignored, and the rates are taken as some macroscopically averaged surface coverage at that reaction condition. Although the present kinetic rate models offer a good qualitative understanding of the kinetics for acetylene hydrogenation, they are nevertheless limited because they are empirical in nature and hold only under the condition for which they have been determined. They ignore the local composition and surface coverage, in addition the influence of heterogeneous (different) reaction sites.

Atomistic simulation can begin to overcome a number of the limitations of conventional deterministic models in that they can track molecular-level transformations and retain the specific atomic surface structure. This enables one to readily include different reactive surface sites based on differences in their atomic surface structure as well as the influence of the

local reaction environment at these sites. We have recently developed and applied first-principle-based kinetic Monte Carlo simulation to model various different catalytic systems, including ethylene hydrogenation, vinyl acetate synthesis, and NO_x reduction [1–4,33–36]. This approach allows for the explicit connection between the atomic surface structure, the dynamics of the surface adlayer, and macroscopically measurable quantities, thus providing the ability to follow multiple reactions over multiple sites. The detailed reaction paths available for each of the different surface intermediates, as well as the influence of the atomic surface structure, can in principle be established from fundamental surface science experiments or from ab initio quantum mechanical calculations. This provides the kinetic data needed for the detailed site-explicit kinetic Monte Carlo simulation. The simulations can ultimately track the temporal changes in molecular adlayer on the surface and the desorption of reaction products, thus enabling the determination of the turnover frequency, reaction selectivity, and the overall reaction order with respect to a particular reactant.

Kinetic Monte Carlo simulation has been used to study various catalytic hydrogenation systems. For example, Duca et al. examined the activity of ethylene hydrogenation over Pt as well as Pd surfaces [37–40], and McLeod and Gladden used this approach to simulate discontinuities in the hydrogenation of hydrocarbons on the Pd(100) surface [41,42]. Both of these studies utilized a lattice gas model along with experimentally determined pre-exponential factors and activation energies. First-principles theoretical methods have now reached the stage whereby they can be used to complement these studies by providing intrinsic kinetic information, thus avoiding the use of empirical kinetic data. We have recently developed a kinetic Monte Carlo algorithm wherein the adsorption energies, overall reaction energies, and activation barriers were derived from first-principle density functional theory (DFT) calculations for various different reaction systems [1–4,33,34,36,43]. The results for different reaction intermediates were directly incorporated into the simulation. The effects of the local environment were treated using a van der Waals interaction model to determine the local steric interactions and longer-range electronic interactions and a bond order conservation (BOC) interaction model to determine the local *through-surface* interactions between adsorbates. These simulations can now be used to follow different elementary reactions occurring over a multisite catalytic surface.

In this paper, we describe the application of this approach to acetylene hydrogenation over Pd(111). Before reporting on our results, however, we first describe the essential features of the kinetic Monte Carlo algorithm used herein.

It should be noted that the catalytic hydrogenation of acetylene over supported Pd is rather complex, involving changes in the adlayer as well as changes in the composition of the metal particles. The presence and the roles of α- and β-hydride, as well as the formation and presence of carbides, are known to influence both activity and selectivity [13,44–46]. In the present work, we focus solely on ideal model Pd(111) surface. Although we account for the influence of surface hydrogen on the reaction kinetics, we do not simulate the formation or presence of α- or β-Pd-hydrides or Pd-carbides. Previous ab initio simulations found that the presence of subsurface hydrogen did not influence the hydrogenation kinetics beyond the increases that were already present due to the higher surface coverages of hydrogen [31]. In addition, we do not follow acetylene oligomerization or decomposition pathways. These are the topics of future efforts.

2. Simulation methodology

2.1. Reaction mechanism model

As discussed above, the chemistry and the kinetics for acetylene hydrogenation can generally be described by a Horiuti–Polanyi-like mechanism involving consecutive hydrogenation steps [18]. Most of the previous experimental results over Pd and Pt catalysts indicate that acetylene hydrogenation likely occurs through a series of successive hydrogenation addition steps rather than through simultaneous direct molecular hydrogenation steps [13–17].

The reaction cycle proceeds by the chemisorption of both acetylene and hydrogen. Acetylene prefers to bind at the three-fold fcc adsorption site on Pd(111) [31]. Hydrogen adsorbs dissociatively, requiring at least two neighboring empty surface sites (three-fold hollow sites or two-fold bridge sites). More recent results by Mitsui et al. indicate that the activation of hydrogen actually may occur through aggregates of three or more sites on Pd(111) [47,48]. The atomic hydrogen thus produced can subsequently react with an adsorbed acetylene molecule to form the vinyl intermediate. The vinyl that forms prefers to sit at the three-fold fcc hollow site in an η^1–η^2 orientation on the Pd(111) surface [31]. It can then either react with a second hydrogen atom to form ethylene or decompose back to form acetylene and atomic hydrogen on the surface. Our theoretical results suggest that the decomposition of vinyl back to the acetylene and atomic hydrogen is favored. Any ethylene that forms binds at either a two-fold bridge site (di-σ position) or an atop site (π position) on the Pd(111) surface. The di-σ intermediate tends to be more stable at lower surface coverages, whereas the π-bound intermediate predominates at higher coverage [49]. Ethylene can either desorb from the surface or react with an additional surface hydrogen atom to form an atop-adsorbed ethyl intermediate. The ethyl intermediate subsequently reacts with atomic hydrogen to produce ethane, which readily desorbs from the surface or dehydrogenates back to form ethylene and atomic hydrogen.

The elementary reaction steps listed in Scheme 1 are used to simulate the controlling hydrogenation reaction kinetics. Subsequent dehydrogenation pathways also can be important, especially if the hydrogen partial pressure is low. Our results demonstrate that these paths ultimately lead to the formation of ethylidyne as the most abundant surface intermediate. We find that ethylidyne tends to block Pd sites but has very little effect on the intrinsic kinetics. We also would not expect to see significant changes in the kinetics, because the hydrogenation of many hydrocarbons is typically structure-insensitive. There are changes in the selectivity, however. At lower hydrogen par-

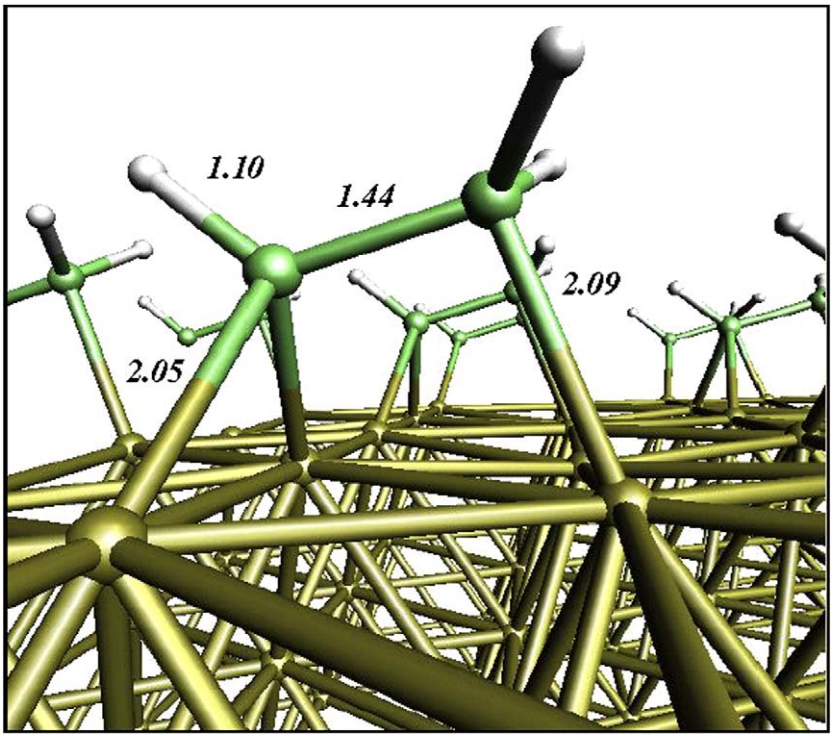

Fig. 1. DFT optimized structure for vinyl adsorbed over Pd(111) in the η_1–η_2 mode (over the three-fold hollow site).

tial pressures, it has been demonstrated that vinylidene rather than ethylidyne covers the surface [5,23,28]. Vinylidene has a higher surface saturation coverage and may have a greater influence on the kinetics. We are currently calculating the paths that lead to the formation of vinylidene and its influence on the kinetics; however, this work is still in progress. Therefore, to focus on the most relevant hydrogenation steps, we do not include these decomposition paths here. We will present a more complete analysis of the decomposition pathways to ethylidyne and vinylidene, and their influence on hydrogenation, in a future communication.

2.2. Intrinsic kinetics database

A comprehensive set of periodic DFT calculations using plane-wave basis sets was performed to establish an intrinsic kinetic database for the selective hydrogenation of acetylene [31]. The database includes ab initio calculated binding energies for all of the reactants, intermediates, and products, along with the activation barriers and the overall reaction energies for all of the elementary reaction steps considered in the mechanism. The errors associated with adsorption energies derived from DFT calculations are typically on the order of 5–8 kcal/mol [50]. This typically leads to activation barriers with similar accuracies. However, the presence of systematic deviations can lead to greater accuracies in overall reaction energies and activation barriers when comparing similar reaction steps, trends, or simulated apparent kinetics. This can be due in part to a cancellation of errors.

All calculations reported herein were carried out using VASP, a gradient-corrected plane wave DFT code developed by Kresse and Hafner [51]. The binding energy for an adsorbate is defined as the difference in the energy between the adsorbed system (adsorbate and surface) and the base energies of the gas-phase adsorbate and the clean metal slab,

$$E_{\text{binding}} = E_{\text{adsorbed system}} - (E_{\text{adsorbate}} + E_{\text{metal slab}}). \quad (9)$$

Fig. 1 shows a representative result, the adsorption of the vinyl intermediate in the η_1–η_2 mode across the three-fold hollow fcc site. This is found to be the most energetically favorable site for adsorbed vinyl, which is consistent with experimental evidence reported by Azad et al. [23]. The binding energy for the vinyl intermediate in a 2×2 overlayer on the Pd(111) was calculated as -65.5 kcal/mol. Table 1 gives the DFT-calculated binding energies for all of the adsorbates considered in this study bound to various different sites on the Pd(111) surface along with their atomization energies. The details of the calculations can be found in a previous publication [31].

Table 1
DFT calculated atomization energies and adsorption energies for all of the different surface intermediates formed over Pd(111) during the hydrogenation of acetylene according to the reaction scheme presented in Eqs. (1)–(8)

Species	Atomization energy (kcal/mol)	Binding energy (kcal/mol)		
		Atop	Bridge	Hollow
Hydrogen (H)	–	−51.6	−58.5	−62.1
Acetylene	417.3	−13.1	−32.7	−41.1
Vinyl	455.7	–	–	−65.5
Ethylene	573.2	−7.0	−14.0	–
Ethyl	613.2	−31.0	–	–
Ethane	674.0	−4.2	–	–
Hydrogen (H_2)	104.2	−1.8	–	–

The intrinsic activation barriers were calculated using the nudged elastic band method [52]. From transition state theory, the difference in the energy between the transition state and that of the reactant state is taken as the activation energy. Fig. 2a shows the intrinsic potential energy diagram for acetylene hydrogenation to ethylene over the Pd(111) surface. The activation barrier for acetylene hydrogenation to vinyl was calculated as +14.9 kcal/mol, whereas the overall reaction energy was exothermic (−6.2 kcal/mol) at a coverage of 25%. Similarly, the intrinsic activation barrier for vinyl hydrogenation to ethylene was calculated as +18.6 kcal/mol, with an overall reaction energy of −13.9 kcal/mol. The DFT results for the intrinsic activation barriers and reaction energies for ethylene hydrogenation to ethane are shown in Fig. 2b. It should be noted that the elementary reaction energies are affected by surface coverage. For example, the activation barrier for acetylene hydrogenation to vinyl decreases from +14.9 kcal/mol at 25% surface coverage to 12.0 kcal/mol at 33% surface coverage, whereas the overall reaction energy changes from −6.2 to −10.3 kcal/mol. The barrier for vinyl hydrogenation to form ethylene decreases from 18.6 to 17.5 as the coverage is increased from 25 to 33%. This indicates that the surface coverage (i.e., the local environment) significantly affects the surface kinetics. Any change in the activation barriers for elementary reaction processes could lead to significant changes in the overall selectivity and macroscopic kinetics. The comparable kinetic values for different hydrogenation steps in the acetylene hydrogenation reaction call for a model to describe the influence of local environment on reaction kinetics.

2.3. Interaction model

The reaction energies are specifically influenced by the local environment around the reaction site. The intrinsic kinetics database was calculated at low coverage to minimize the interaction between adsorbates. Subsequent calculations at higher coverage were carried out to appropriately model the influence of the local environment on the reaction kinetics. The results were used to parameterize a more coarse-grained models that are called on internally within the simulation to provide estimates of the adsorbate–adsorbate interactions, thus providing a more quantitative analysis of the influence of the local reaction environment. We classify adsorbate–adsorbate interactions at the surface into two general categories: *through-space* and *through-surface*. *Through-space* interactions are the result of direct steric interactions or long-range electronic interactions between different surface intermediates. The *through-space* interactions are calculated in-situ in the simulation by using the van der Waals interaction term from the Merck molecular force field (MMFF) model [53,54]. *Through-surface* interactions arise from metal-atom sharing or adsorbate-bond sharing and are estimated by using a DFT-scaled bond order conservation (BOC) model [1–4,33,35,36] developed previously. The BOC model was parameterized against DFT results carried out at various coverages. Note that any longer-range electronic interactions would be implicitly incorporated in the BOC model, because this model was regressed against different coverage DFT values. The MMFF model treats the cooperative van der Waals interactions that might exist through long-range adsorbate networks. This has been described in more detail previously [1–4,33,35,36].

The energetics/kinetics database is subsequently used to calculate reaction rates. The reaction rate for each elementary step is calculated using transition state theory, with the rate given by

$$r_i = \nu_i \exp\left(-\frac{\Delta E_i}{RT}\right), \tag{10}$$

where ν_i is the pre-exponential factor, R is the gas constant, T is the temperature, and ΔE_i is the activation barrier for the elementary reaction i. The pre-exponential factor ν_i can be calculated directly from DFT calculations or from statistical mechanics estimates. The barriers for individual elementary steps were determined by DFT calculations. The pre-exponential factors, ν_i, were chosen herein to be standard statistical mechanical estimates for surface processes. For unimolecular surface reactions and (immobile) bimolecular reactions, the pre-exponential factors were calculated to be 10^{13} s^{-1} [55]. The pre-exponential factors for desorption were also estimated from statistical mechanical estimates to be on the order of 10^{13}. Note that the simulated results were not significantly affected by changes in the pre-exponential factors [55].

The calculation of the adsorption rate is characteristically different from that of the surface elementary reaction rate. The adsorption rate for species i is defined as [2,4,33,35]

$$r_{\mathrm{ad,i}} = s_0 \cdot P_i \cdot A_{\mathrm{S}} \cdot (2\pi \cdot MW_i \cdot RT)^{-0.5} \cdot \exp\left(-\frac{\Delta E_i}{RT}\right), \tag{11}$$

where s_0 is the sticking coefficient, P_i is the partial pressure of species i, A_s is the area of one surface site, and MW_i is the molecular weight of species i. The estimation of sticking coefficients would require simulations of dynamics. Classical molecular dynamics would be very approximate because of the lack of accurate interatomic potentials to describe the adsorbate interactions with the surface. Ab initio molecular dynamics could be used to simulate sticking coefficients, but this would require sampling many different trajectories, which is beyond the scope of this work. Instead, we take the sticking coefficients of acetylene and hydrogen to be 1.0 and 0.1, respectively, based on previous fundamental experimental studies [56,57].

2.4. Kinetic Monte Carlo approach

The kinetic Monte Carlo simulation that we have developed can be used to explicitly track individual molecular transformations as functions of time and processing conditions [33,35,55,58–60]. We briefly describe our approach below. Herein we simulate the (111) surface, which is represented by a periodic 32 × 32 Pd atom lattice containing 4096 different surface sites including atop, bridge, and three-fold hollow sites. The structural, energetic, and kinetic properties that compose the kinetics database are used as input to the simulation. Molecular information, such as the binding energies and molecular geometries of the adsorbates at all possible adsorption sites, van der Waals

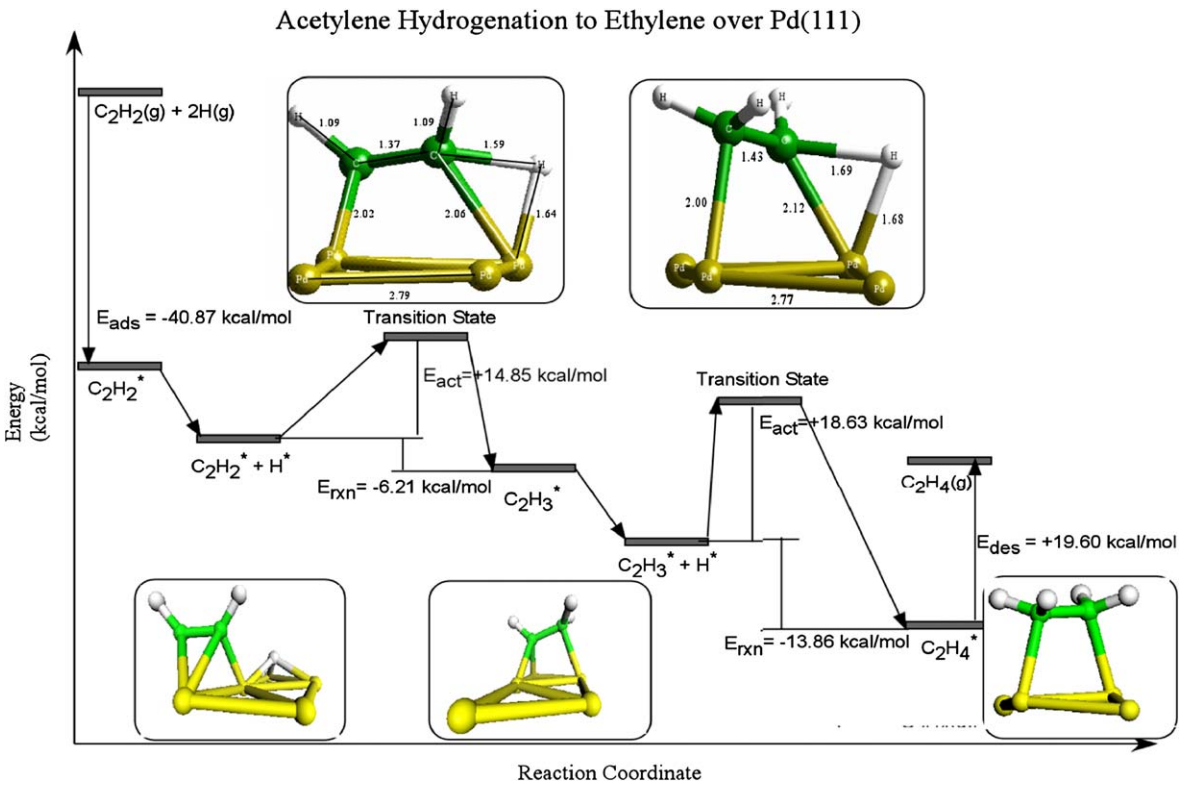

(a)

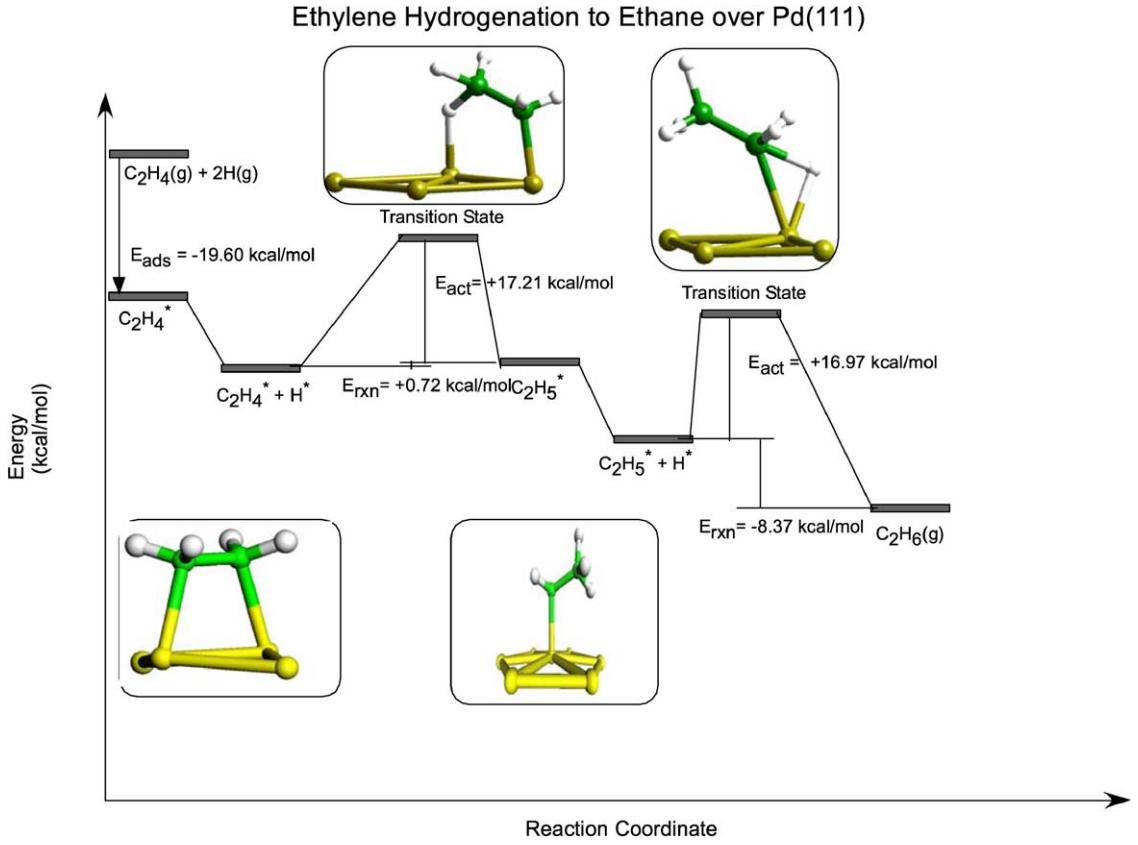

(b)

Fig. 2. DFT calculated overall reaction energy diagram for the hydrogenation of: (a) acetylene to ethylene and (b) ethylene to ethane.

radii (physical size), and the dissociation energies of all possible reactants, intermediates, and products, is also included as input. The intrinsic kinetic database obtained from the DFT results is subsequently combined with the through-surface and through-space adsorbate models to describe the influence of the reaction environment. This forms the core reaction model used within the variable time step kinetic Monte Carlo algorithm to simulate reactivity. After initialization, all of the sites on the surface are randomly sampled to construct an overall cumulative reaction probability distribution that defines all possible kinetic events that can occur at that particular point in time, t_i, including adsorption, surface reaction, surface diffusion, and desorption steps. The events considered depend on the specific site for the event as well as on its surrounding reaction environment. For each surface reaction event, we calculate the binding energies for all reactants as well as possible product states to determine the overall reaction and chemisorption energies along with the influence of the reaction environment on each step. The *intrinsic* activation barriers are taken from the DFT results that make up the kinetics database. The *apparent* activation barrier is determined in situ by calculating the through-surface and through-space interactions from the semiempirical BOC and van der Waals models described above. The number of local intermediates, their types, and their specific locations within the active sites are used in calculating these adsorbate interactions.

At any instant in time, t_i, the rates for all possible events are added together to determine the total rate. The total rate of all possible surface events is calculated by summing all possible surface reaction rates, $\sum r_i$. The total rate is subsequently used along with the variable time-step equation given below to determine the time step at which some possible event on the surface will occur,

$$\Delta t_{\mathrm{v}} = -\frac{\ln(RN)}{\sum_i r_i}, \tag{12}$$

where Δt_{v} is the variable time step and RN is a random number between 0 and 1. The total time is updated by adding the calculated variable time step (Δt_{v}) to the current time (t_i). The specific reaction occurring within the calculated time step interval is then chosen by comparing the cumulative reaction probability distribution given below against another random number chosen between 0 and 1,

$$P_i = \frac{r_i}{\sum_i r_i}. \tag{13}$$

If the random number chosen is between P_{i-1} and P_i, then event i is chosen as the reaction event. The simulation then proceeds event by event, updating the time as well as the surface structure, surface composition, and gas-phase products after each event. The outcome from the simulation includes the detailed structure and composition of the adlayer as functions of time and processing conditions. This temporal and spatial resolution of the surface enables us to compute a range of properties, including molecular- or site-explicit turnover frequencies (TOFs), activation barriers, surface coverages, and overall averaged properties.

3. Results and discussion

The simulations reported herein were carried out in both the presence and the absence of lateral interactions to determine the influence of the interactions on the kinetics. The MMFF-BOC models described above were used to simulate these interactions. To "turn off" the lateral interactions, the MMFF-BOC interactions were set to zero, and the model was replaced with a simple hard sphere model that acts only to prevent adsorbates from occupying the exact same sites.

3.1. Hydrogenation kinetics

A series of kinetic Monte Carlo simulations for the selective hydrogenation of acetylene was performed at different temperatures ranging from 300 to 500 K over the well-defined Pd(111) surface to probe the apparent reaction kinetics as well as the overall selectivity. The partial pressures of acetylene and hydrogen in the gas phase were both set constant at 100 Torr. The simulation conditions were chosen to mimic those of the experiments of Molero et al. [5] for hydrogenation over Pd to compare the simulation results with those from the experiments. Each simulation was allowed to equilibrate to a steady state in which all of the surface coverages for all of surface intermediates reached constant values, with the exception of small fluctuations resulting from the stochastic nature of the simulation. After achieving steady state, the overall macroscopic kinetic values, such as the TOF, average surface coverage, and average binding energy for all surface intermediates were calculated. The TOFs for ethylene and ethane production were calculated by simply counting the number of ethylene and ethane molecules desorbing from the surface in a given time interval. The number of molecular desorption events as a function of time was fit to a simple function that includes a first-order exponential term to describe the initial transient unsteady-state kinetics, followed by a straight line to model the long-time steady-state behavior. The TOF values reported herein were determined from the long-term behavior, in which the slope of the straight line was normalized based on the total number of surface Pd atoms. The long-term time of the simulations varies depending on the specific conditions, but the steady-state is typically realized somewhere between 0.01 and 10 s.

As expected, the TOFs for ethylene and ethane formation increase with increasing temperature. Fig. 3 compares our simulation results for the TOF at steady state as a function of temperature with experimentally measured TOF values [5]. The simulation results closely match the experimental results, especially considering that the kinetics were derived from first principles without any experimental data, with the exception of the sticking coefficients, which were taken from general surface science studies over model single-crystal surfaces. The calculated TOFs at different temperatures closely match those reported experimentally over model Pd(111) surfaces [5]. The apparent activation energy for acetylene hydrogenation is 8.0 ± 0.6 kcal/mol, as determined by fitting the logarithm of TOF values for ethylene production with respect to the reciprocal of temperature in a classical Arrhenius power law expression. Note that this *appar-*

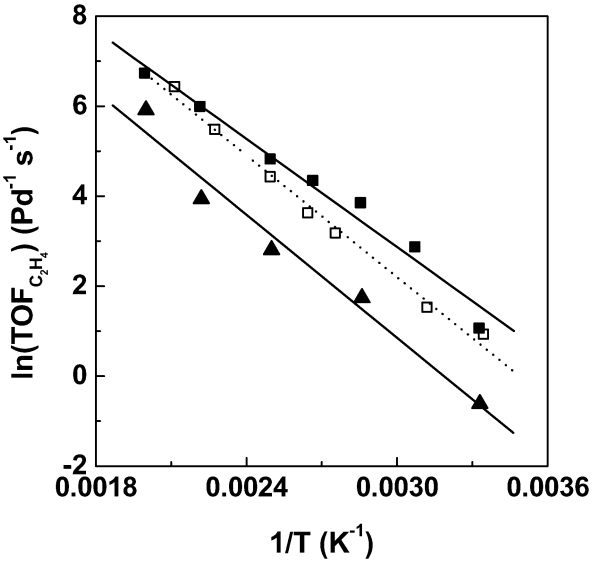

Fig. 3. Comparison between the simulated and experimental results for the temperature dependence of the turnover frequencies of acetylene hydrogenation over Pd(111). (■) Simulation results using the full MMFF-BOC lateral interaction model; (▲) simulation results using the non-interacting hard-sphere model; (□) experimental data [5], (—) best line fit for each case. The slopes of the corresponding Arrhenius plots represent the respective apparent activation energies for acetylene hydrogenation over Pd(111).

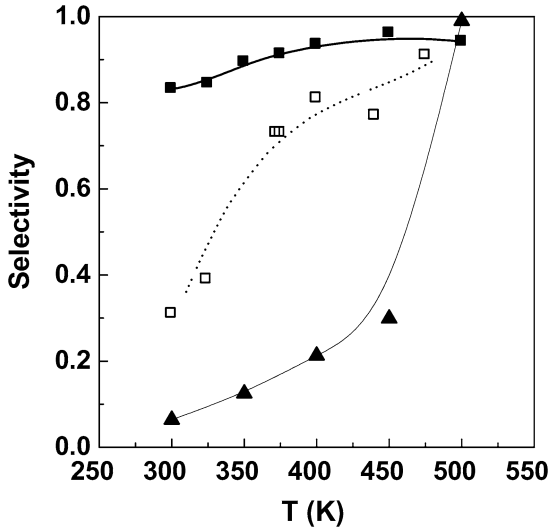

Fig. 4. Comparison between the simulated and experimental results for the temperature dependence of the ethylene formation selectivity over Pd(111). (■) Simulation results using the full MMFF-BOC lateral interaction model; (▲) simulation results using the non-interacting hard-sphere model; (□) experimental data [5].

ent activation energy differs from the elementary step activation barriers determined from DFT calculations shown in Fig. 2. The simulated apparent activation energy for acetylene hydrogenation over Pd(111) surface compares reasonably well with the experimentally apparent activation energy of 9.6±0.1 kcal/mol over a clean Pd foil under the same conditions reported by Molero et al. [5]. The simulated apparent activation energy also agrees with previous experimental results over supported particles, ranging from 9.7 to 11.6 kcal/mol, depending on the experimental conditions used and the actual preparation and conditioning of the catalyst [12,15,61,62].

Hard-sphere simulations were subsequently carried out in which all of the lateral interactions (both through-surface and through-space) were turned off, to compare them with the results from the full simulation, including lateral interactions. The results, shown in Fig. 3, indicate that the reported TOFs are considerably lower than those from the MMFF-BOC model, as well as those from experiments. The calculated apparent activation barrier increases slightly, from 8.0 to 9.1 kcal/mol, when the lateral interactions are removed. This relatively small influence on the barrier can be attributed to the fact that the kinetics for hydrogenation tends to be structure-insensitive. The acetylene- and hydrogen-binding energies are significantly weaker for the MMFF-BOC model than those found in the hard sphere model. This is due to the fact that the lateral interactions in the MMFF-BOC model are predominantly repulsive, which weakens the adsorbate–surface bonds. The hard-sphere model, on the other hand, simply ignores the lateral interactions, resulting in greater adsorbate-binding energies. The higher binding energies for the hard-sphere model leads to stronger metal–hydrogen and metal–carbon bonds in the transition state, resulting in increased intrinsic barriers for hydrogenation and thus a slightly higher overall apparent activation barrier. The increased hydrogen coverage in the hard sphere model can begin to compensate for the increased activation barrier by increasing the available hydrogen at the surface. The changes in the net rate remain quite similar, however.

The selectivity to ethylene production is defined as follows:

$$S = \frac{\mathrm{TOF}_{\mathrm{ethylene}}}{\mathrm{TOF}_{\mathrm{ethylene}} + \mathrm{TOF}_{\mathrm{ethane}}}. \tag{14}$$

Ethylene selectivity for the full simulations (which include lateral interactions) increases from 82 to 94% as the temperature increases from 300 to 500 K. This agrees qualitatively with the experimental results shown in Fig. 4, but with some notable quantitative differences, largely due to the limited set of unselective reaction pathways and side products included in the present simulation. Selectivity is defined in the experiments [5] as the ratio between the rate of ethylene formation to the rate of formation of all products, including ethylene, ethane, C_4 products, and benzene. The current simulations, however, do not include other reaction processes, such as oligomerization reactions, that would lead to C_4 intermediates, cyclotrimerization, and benzene formation. These additional paths can lead to appreciable byproducts and thus lower the selectivity at lower temperatures. Molero et al. reported a significant increase in selectivity with increasing temperature from about 30% at 300 K to about 94% at 470 K [5]. The increase in selectivity with temperature, which is seen in the simulations as well as in the experiments, can be rationalized by recognizing that although the rates of acetylene hydrogenation and ethylene hydrogenation both increase with increasing temperature, the desorption rate of ethylene increases faster than that of ethylene hydrogenation with increasing temperature. Another reason for the increased selectivity with temperature is the result of changes in the specific surface coverage with changes in temperature that result from the elementary surface kinetics.

The change in selectivity with temperature for the full simulations was found to be very different than the change for simulations carried out in the absence of lateral interactions. In the non-interacting hard-sphere model, the selectivity at low temperature was found to be rather low. At 300 K, the selectivity to ethylene was only 30%. The lower selectivity is the result of (1) the overbonding of ethylene at low temperatures, due to the absence of all repulsive interactions, and (2) an overabundance of hydrogen on the surface for the hard-sphere simulations, which enhances the subsequent hydrogenation steps and promotes overhydrogenation. The simulated selectivity from the hard-sphere model increases toward 85% as the temperature is increased to 500 K. It is clear from Fig. 4 that the selectivity is much more sensitive to surface coverage and the presence of lateral interactions than the overall activity. The lower surface coverages resulting from the simulations that explicitly include lateral interactions tend to minimize overhydrogenation. The simulations carried out with the hard-sphere model resulted in much higher surface coverages and overhydrogenation, especially at temperatures below 450 K.

The overall kinetics is controlled not only by the intrinsic rate constant, but also by the surface coverage. The simulations allow us to explicitly track the identity and specific transformations for each surface species, as well as the average surface composition of different intermediates as functions of time and processing conditions. This information is subsequently used to establish the influence of specific intermediates on the kinetics. The average surface coverages for atomic hydrogen and acetylene as a function of temperature are plotted in Fig. 5. The full simulations, which include lateral interactions, result in hydrogen surface coverage close to 0.06 ML at 300 K, as shown in Fig. 5a. As the temperature increases, the hydrogen atoms on the surface recombine to form H_2, which desorbs from the surface. At 500 K, for example, the hydrogen surface coverage decreases to 0.005 ML. The hydrogen surface coverage from the non-interacting hard-sphere simulations is significantly higher, 0.36 ML at 300 K, decreasing to 0.07 ML at 500 K. These differences ultimately control the availability of hydrogen and thus influence both the rate and selectivity of the reaction.

The surface coverage of acetylene exhibits an opposite trend with temperature, as shown in Fig. 5b, increasing from 0.332 to 0.365 ML over the same temperature range. The increased desorption of hydrogen with temperature leads to more vacant surface sites, which increases the binding of acetylene on the surface and subsequently leads to increased acetylene surface coverage with temperature. The increase is small, because higher temperatures also enhance the desorption and hydrogenation of acetylene from the surface. At higher temperatures, the increase in acetylene uptake decreases.

In the absence of lateral interactions (i.e., the hard-sphere model), the acetylene surface coverage decreases from 0.55 to 0.37 ML as the temperature increases from 300 to 500 K. The higher coverage of acetylene at low temperature is due to the fact that we have ignored all repulsive interactions within this model. Higher temperatures subsequently lead to acetylene desorption or hydrogenation from the surface.

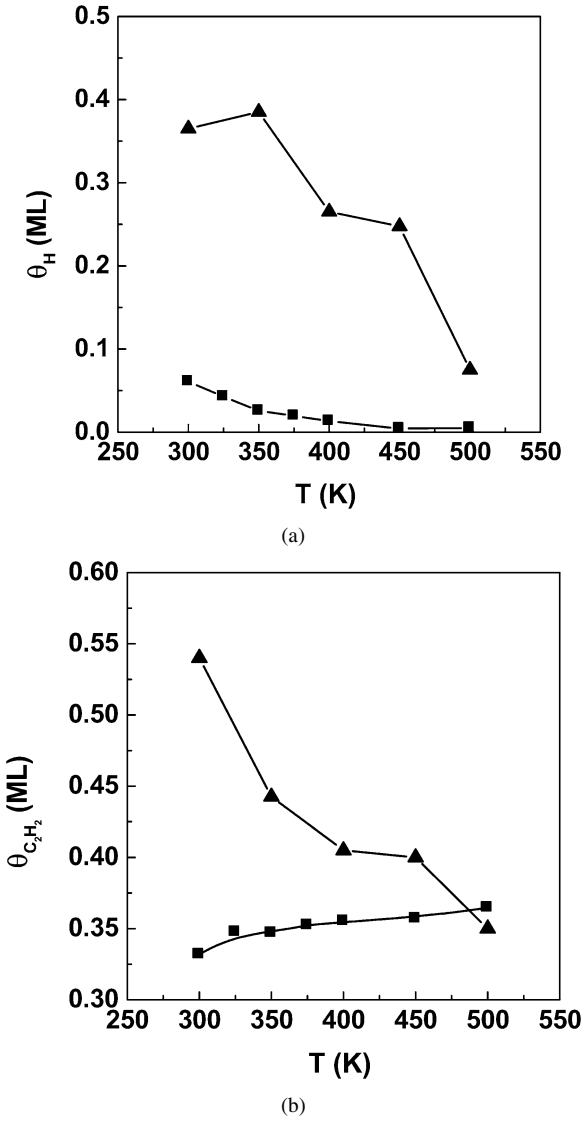

Fig. 5. Kinetic Monte Carlo simulation results for the temperature dependence of the surface coverage of (a) hydrogen; and (b) acetylene during the steady state hydrogenation of acetylene over Pd(111). (■) MMFF-BOC lateral interaction model; (▲) non-interacting hard-sphere model.

The coverages of vinyl, ethylene, and ethyl are generally very low at the temperatures examined. These intermediates have very short residence times on the surface regardless of whether or not the simulations include lateral interactions. The surface is covered predominantly with acetylene over all of the temperatures examined, whereas the hydrogen surface coverage is limited. Surface hydrogen atoms react rapidly with acetylene and other hydrocarbon intermediates. However, the availability of acetylene and hydrogen on the surface limits the rates of all hydrogenation steps. The ethylene surface coverage is also quite low. The ethylene formed from acetylene hydrogenation desorbs readily from the surface or hydrogenates further to form ethane. This relatively weak adsorption energy of ethylene on Pd promotes both desorption and further hydrogenation. Finally, the surface coverages for vinyl and ethyl intermediates were also quite low. The surface coverages of reaction intermediates for the full simulation results are reported in Table 2.

Table 2
Simulated surface coverages of the reaction intermediates for acetylene hydrogenation over Pd(111) at $P_{C_2H_2} = 100$ Torr and $P_{H_2} = 100$ Torr

	T (K)						
	300	325	350	375	400	450	500
Hydrogen	0.061	0.043	0.026	0.020	0.013	0.004	0.005
Acetylene	0.332	0.348	0.347	0.352	0.355	0.357	0.365
Vinyl	0.001	0.001	0.001	0.001	0.001	0.001	0.001
Ethylene	0.001	0.001	0.001	0.001	0.001	3.1×10^{-5}	3.1×10^{-5}
Ethyl	3.4×10^{-5}	2.1×10^{-5}	9.4×10^{-7}	1.7×10^{-5}	7.6×10^{-6}	1.9×10^{-6}	3.2×10^{-7}

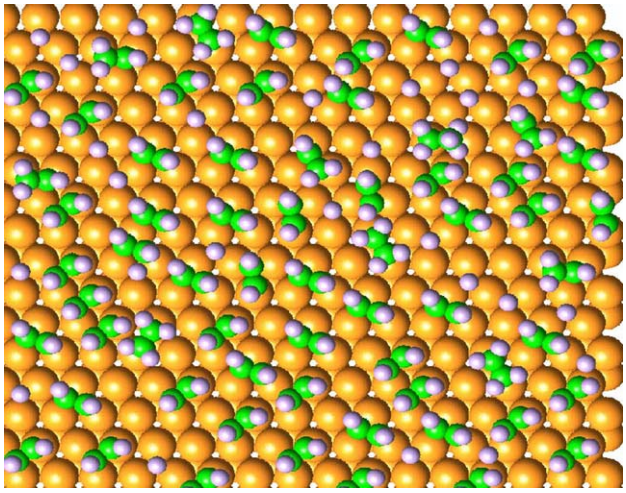

Fig. 6. A snapshot of the Pd(111) surface at some point in time for the steady state kinetic Monte Carlo simulation of acetylene hydrogenation over Pd resulting from the full lateral interaction model.

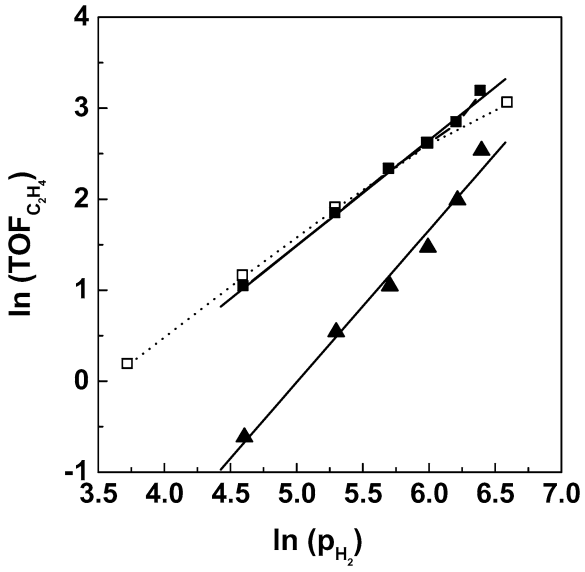

Fig. 7. Comparison between simulated and experimental results for the hydrogen partial pressure dependence of the turnover frequency of acetylene hydrogenation over Pd(111). (■) Simulation results using the full MMFF-BOC lateral interaction model; (▲) simulation results using the non-interacting hard-sphere model; (□) experimental data [5].

Acetylene dominates the surface for all of the reaction conditions studied here.

The results given here suggest that the addition of hydrogen to vinyl is rate-controlling compared with the other elementary reactions. However, first-principles DFT results for the reaction pathways for acetylene hydrogenation have reported that the addition of hydrogen to acetylene and vinyl have comparable activation barriers at low coverage [31]. This would indicate that the coverage effects in the vicinity of the reaction environment are critical in governing the kinetics of acetylene hydrogenation. Previous surface science experiments have suggested that the rate is controlled by the addition of the first hydrogen atom to acetylene; however, this conclusion is based on a comparison of the rates of hydrogenation of preadsorbed acetylene or preadsorbed vinyl from palladium. The surface coverages for acetylene and vinyl in these experiments were taken to be somewhat similar to one another. But our results indicate that under reaction conditions, the surface coverage of vinyl is orders of magnitude lower than that for acetylene. Therefore, even though the activation barriers are similar for the two steps, the TOF for the hydrogenation of vinyl is limited by its very low surface coverage. The large differences in surface coverage were not examined in the UHV studies, however.

In addition to average surface coverage, the simulation can be used to track more of the microscopic details during the simulation. Fig. 6 shows a snapshot of the simulation overlayer structure, illustrating the dominance of acetylene in the total surface coverage. Acetylene, hydrogen, and vinyl are bound in the hollow sites on the surface. Ethylene, on the other hand, typically adsorbs on either the bridge (di-σ position) or the atop sites (π-position). Ethylene is only weakly adsorbed and will readily desorb as the temperature is increased. The ethyl intermediate binds to atop sites but is quickly hydrogenated to ethane or dehydrogenated back to form ethylene. Like ethyl, the vinyl species are also unstable on the surface. Vinyl either reacts quickly with a neighboring hydrogen atom to form ethylene or dissociates back to acetylene and hydrogen due to the low barrier for this reverse reaction. This is in agreement with experimental observations indicating that very few vinyl and ethyl intermediates are detected on the surfaces [23,63,64].

3.2. *Effect of hydrogen partial pressure*

The effect of hydrogen partial pressure on the kinetics for the selective hydrogenation of acetylene has been studied by performing the simulation with different hydrogen partial pressures ranging from 100 to 600 Torr at 300 K and an acetylene partial pressure of 100 Torr. Fig. 7 compares simulation results for the ethylene TOFs with corresponding experimental data [5]. The simulated TOFs for ethylene closely agree with

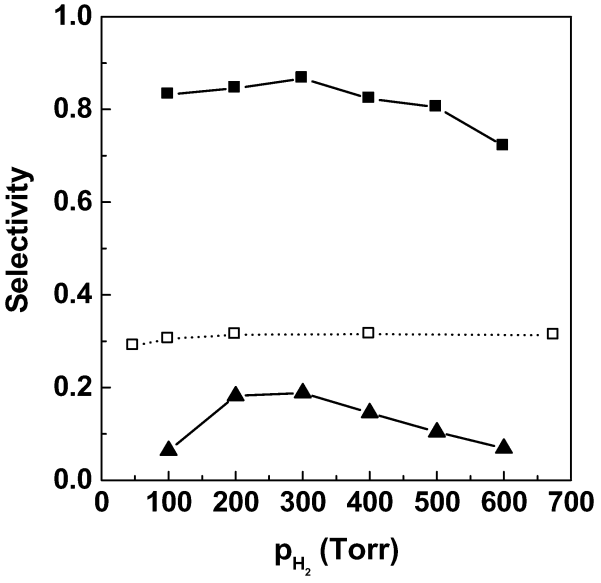

Fig. 8. Comparison between the simulated and experimental results for the hydrogen partial pressure dependence of the selectivity of ethylene formation over Pd(111). (■) Simulation results using the MMFF-BOC lateral interaction model; (▲) simulation results using the non-interacting hard-sphere model; (□) experimental data [5].

the experimental values. By fitting the simulated ethylene TOFs to the rate model shown in Eq. (15), we can then establish the influence of hydrogen partial pressure on the macroscopic rate,

$$r_{C_2H_4}(\mathrm{TOF}) = \nu \cdot \exp\left(-\frac{E_a}{RT}\right) P^x_{C_2H_2} \cdot P^y_{H_2}. \quad (15)$$

The results from the simulations indicate that the hydrogen reaction order is 1.16 ± 0.03. This is in excellent agreement with the reported experimental value of 1.04 ± 0.02 at the same conditions [5]. The simulated hydrogen reaction order also compares very favorably with other previous experimental values, which range from 1.0 to 1.25 over supported Pd catalysts [15,62].

Simulations carried out in the absence of lateral interactions (i.e., the hard-sphere model) resulted in a hydrogen reaction order of 1.6, which is significantly higher than that for the simulations carried out in the presence of lateral interactions (1.16) and those reported experimentally (1.04). In the absence of lateral interactions, the adsorption energies for acetylene, other hydrocarbon intermediates, and hydrogen are stronger. This leads to higher elementary step activation energies, as well as a higher apparent activation barrier and slower kinetics. In the absence of lateral interactions, higher hydrogen coverages are necessary to increase the number of reactive collisions and thus compensate for the higher intrinsic barriers. This thus results in the higher hydrogen reaction order.

Increasing the hydrogen partial pressure not only increases the acetylene hydrogenation rate, but also increases the ethylene hydrogenation rate, which can ultimately influence the selectivity. The hydrogen pressure dependence on selectivity is given in Fig. 8. The selectivity goes through a maximum of 87% at $P_{H_2} = 300$ Torr with respect to the hydrogen pressure. Our simulation results for ethylene selectivities are significantly higher than those reported experimentally [5]. Molero et al. reported that the selectivity to ethylene formation was ∼28% at $P_{H_2} = 50$ Torr, increasing to and plateauing at about 31% for $P_{H_2} = 200$ Torr. Further increases in the hydrogen partial pressure to 600 Torr did not change the selectivity for ethylene production, aside from a slight drop at much higher hydrogen pressures. The difference between the simulation and experimental results is attributed to the formation of benzene and C_4 intermediates during the acetylene hydrogenation reaction in the experimental study, which were not included in the theoretical simulations performed here. Palladium is known to form C_4 and C_6 intermediates and can be quite active for acetylene cyclotrimerization [65–68]. Molero et al. reported that the benzene formation rate also increases linearly with increasing hydrogen partial pressure [5]. The slight drop in the experimental ethylene selectivity is thought to be the result of accelerated benzene formation at higher hydrogen pressures. Our simulations indicate that the higher hydrogen coverage increases ethylene hydrogenation to ethane, which can also contribute to the decrease in selectivity. Fig. 9a shows that hydrogen surface coverage increases from 0.06 to 0.10 ML as the hydrogen partial pressure increases from 100 to 600 Torr. The calculated barriers for the elementary hydrogenation steps outlined in Fig. 2 all appear quite similar [31]; therefore, the rate for each step will be much more dependent on the surface coverages of the reactants, presuming that the rate constant is similar. The Pd surface was covered predominately by acetylene even at higher hydrogen partial pressures. The acetylene surface coverage does decrease slightly from 0.332 to 0.314 ML at higher hydrogen pressure, as shown in Fig. 9b. In this situation, the acetylene coverage has little effect on the hydrogenation reaction rate. However, the hydrogen coverage plays an essential role in controlling the hydrogenation reaction rates and selectivity. An increase in hydrogen surface coverage will enhance the likelihood that ethylene will hydrogenate to form ethyl and then onto ethane.

Simulations carried out using the hard-sphere model, which ignores lateral interactions, show a more pronounced maximum in the selectivity with hydrogen partial pressure, as shown in Fig. 8. The maximum appears at 300 Torr of hydrogen. At hydrogen partial pressures below 300 Torr, the surface appears to be dominated by acetylene as is shown in Figs. 9a and 9b. Between 300 and 500 Torr there is a significant increase in hydrogen surface coverage and a decrease in acetylene surface coverage. This dramatic increase in hydrogen coverage tends to result in the hydrogenation of both acetylene and ethylene, which acts to lower selectivity. The selectivity is significantly lower than that for the results from the full simulations, which include lateral interactions. The selectivity for the non-interacting simulations range from 7 to 19%, whereas that for the simulations that include lateral interactions range from 79 to ∼86%. In summary, increasing the partial pressure of hydrogen increases the hydrogen surface coverage. In both the hard-sphere and full lateral interaction models, the higher hydrogen coverage increases the rate of hydrogenation of acetylene to ethylene, as well as that for the hydrogenation of ethylene to ethane. At lower hydrogen coverage, the first hydrogenation step (from acetylene to ethylene) is faster than the second hydrogenation step (from

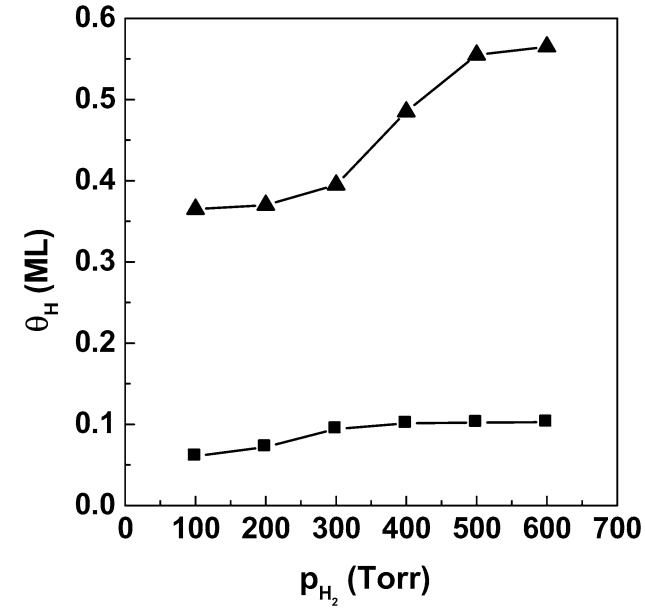

(a)

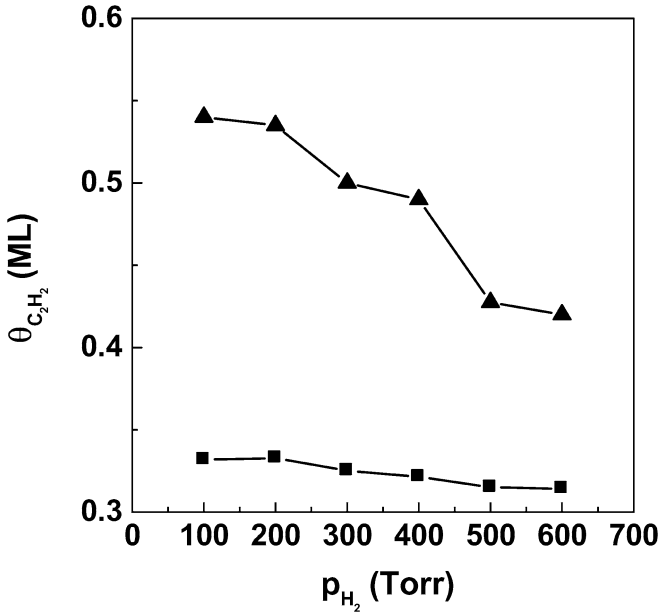

(b)

Fig. 9. Hydrogen partial pressure dependence of the steady-state surface coverage of: (a) hydrogen and (b) acetylene during acetylene hydrogenation over Pd(111). (■) MMFF-BOC lateral interaction model; (▲) non-interacting hard-sphere model.

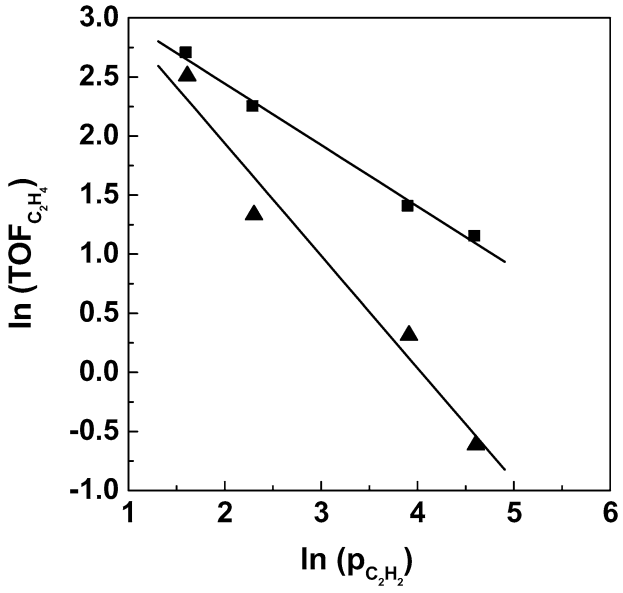

Fig. 10. Acetylene partial pressure dependence of the steady-state turnover frequency for acetylene hydrogenation over Pd(111). (■) MMFF-BOC lateral interaction model; (▲) non-interacting hard-sphere model.

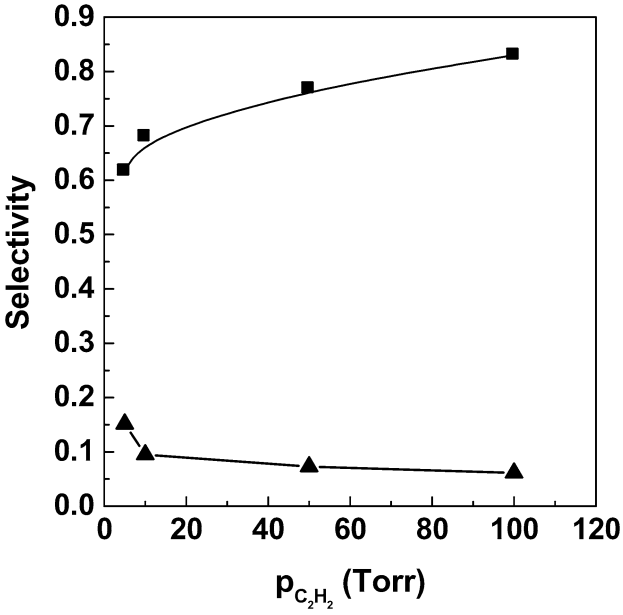

Fig. 11. Acetylene partial pressure dependence of the steady-state selectivity to ethylene formation over Pd(111). (■) MMFF-BOC lateral interaction model; (▲) non-interacting hard-sphere model.

ethylene to ethane), due to the limited hydrogen surface coverage and the lower surface coverage of ethylene. However, increasing the hydrogen availability on the surface increases the rates for both hydrogenation steps nearly equivalently. At this point, the selectivity decreases due to a lower reaction preference.

3.3. Effect of acetylene partial pressure

The effect of the acetylene partial pressure on the kinetics was examined by carrying out simulations at different acetylene partial pressures ranging from 5 to 100 Torr, with the system temperature set at 300 K and the hydrogen partial pressure maintained at 100 Torr. The results, shown in Figs. 10–12, indicate that the rates for both acetylene and ethylene hydrogenation decrease with increasing acetylene partial pressure. The full simulations, which include the lateral interactions, indicate that the TOF for ethylene hydrogenation decreases from approximately 20 to 3.5 s^{-1} as the partial pressure of acetylene is increased from 5 to 100 Torr, as shown in Fig. 10. The full simulations, which include lateral interactions, indicate an acetylene reaction order of -0.52 ± 0.03. This is in

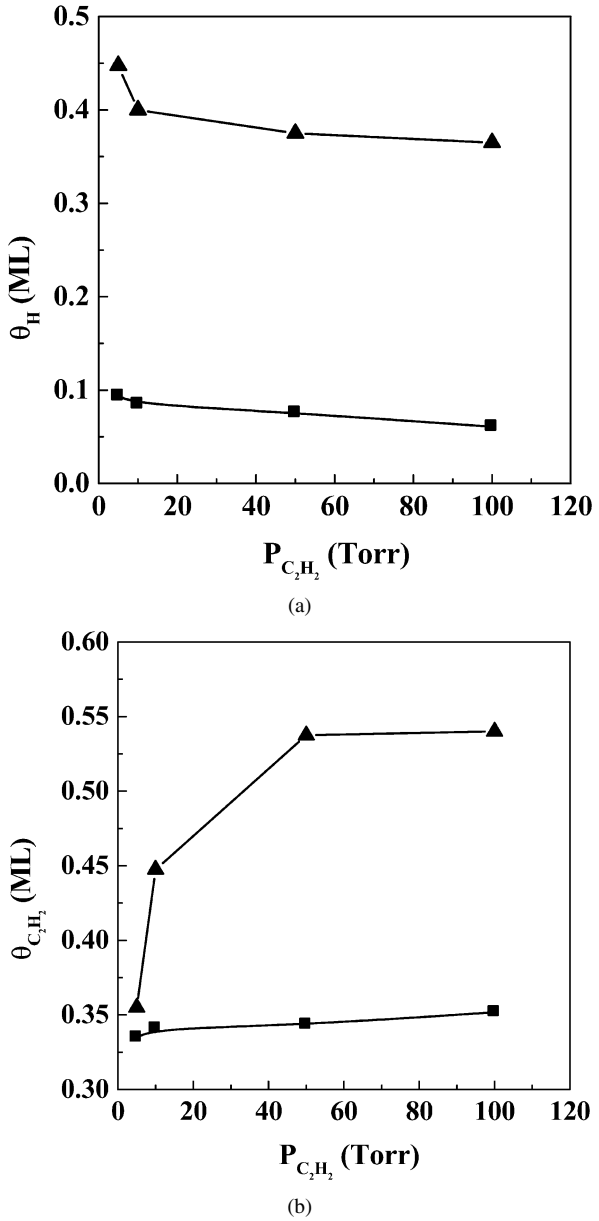

Fig. 12. Acetylene partial pressure dependence of the steady-state surface coverage of (a) hydrogen and (b) acetylene during acetylene hydrogenation over Pd(111). (■) MMFF-BOC lateral interaction model; (▲) non-interacting hard-sphere model.

good agreement with the corresponding experimental value of -0.66 ± 0.02 [5]. The acetylene reaction order also agrees with other experimental acetylene orders, which fall between -0.4 and -0.6 over Pd foil [62] and between -0.55 and -0.67 over Pd supported on alumina [15].

The TOF is significantly greater for the full simulations than for the simulations carried out using the non-interacting hard-sphere model. A much stronger poisoning effect occurs in the hard-sphere simulations than in the full simulations. Acetylene is more strongly bound to the surface in the hard-sphere simulations due to the absence of repulsive interactions; this blocks sites for hydrogen adsorption, significantly lowering the surface coverage of hydrogen as well as the rate of hydrogenation with increasing acetylene partial pressure. Consequently, the acetylene reaction order decreases from -0.52 for the full simulations with lateral interactions to -0.95 for the hard-sphere simulations. In the full simulations, the binding energy for acetylene is weaker as the result of the repulsive lateral interactions. These interactions lower the barrier for hydrogenation, which partially compensates for the loss of hydrogen from the surface. But the rate of hydrogenation is still suppressed by the increased coverage of acetylene, which drives hydrogen from the surface and blocks sites on the surface.

Fig. 11 shows the effect of acetylene partial pressure on selectivity to the ethylene product. The selectivity in the full lateral interaction simulations increases from 0.62 to 0.83 with increasing acetylene partial pressure. This agrees qualitatively with experimental observations reported by Bond and Wells [15] that the selectivity for ethylene production increased from 0.92 to 0.96 with increasing acetylene pressure from about 20 to 150 Torr at 273 K over alumina supported Pd. The negative order in acetylene indicates that acetylene strongly adsorbs and blocks active surface sites and thus limits the amount of surface hydrogen. As the acetylene partial pressure is increased, the acetylene surface coverage increases slightly, from 0.33 to 0.35 ML (see Fig. 12a), and the hydrogen surface coverage decreases correspondingly, from 0.09 to 0.06 ML (see Fig. 12b). The lower hydrogen coverage at higher acetylene pressure causes the ethylene hydrogenation step to be less likely, due to the decreased amount of available nearby hydrogen adatoms. Consequently, ethylene will prefer to desorb rather than undergo further hydrogenation. As a result, the selectivity increases with increasing acetylene partial pressure. Again, the hydrogen surface coverage has a significant affect on the selectivity of acetylene hydrogenation over the Pd(111) surface.

The acetylene reaction order identified from the hard-sphere simulations (without lateral interactions) is -0.95, which is significantly lower than that calculated from the full simulations (-0.52). This decrease in the acetylene reaction order is due to the much higher coverages found in the hard-sphere simulations. Both the hydrogen and the acetylene coverages are substantially higher in the hard-sphere simulations, leading to a much greater degree of inhibition. The hydrogen coverage decreases from 0.45 to 0.37 ML as the partial pressure of acetylene increases from 5 to 100 Torr as acetylene displaces hydrogen from the surface (see Figs. 12a and 12b). This effect is greater for the hard-sphere simulations, which ignore lateral interactions. This ultimately results in more negative acetylene reaction orders.

3.4. Rate determination

By tracking the time at which each reaction proceeds, we can calculate the actual rate for each elementary step. This requires that we average over sufficiently large ensembles to provide relatively accurate statistics. The averaged rates for the forward and reverse processes that compose the mechanism outlined in Eqs. (1)–(8) are shown in Fig. 13. Herein we examine only the rates from the full simulation results. Two different overall rate processes appear to control the kinetics. The steps associated

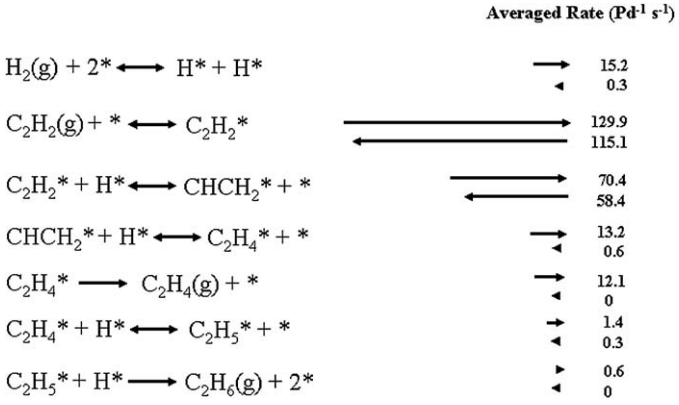

Fig. 13. A comparison of the average steady-state reaction rates for the forward and reverse steps for all of the elementary steps considered in the simulation of acetylene hydrogenation over Pd(111).

with acetylene hydrogenation (steps 1–5) occur at an overall average of 12–23 reactions per surface Pd atom per second. Ethylene readily desorbs from the surface, so the overall rate for ethylene hydrogenation is characteristically lower because it requires readsorption. These steps occur at an overall average rate of 0.6–1.1 reactions per surface Pd atom per second. An analysis of the rates of individual steps indicates that ethylene adsorption and hydrogenation of acetylene to vinyl are quasi-equilibrated with respect to time. Hydrogen adsorption, hydrogenation of vinyl to ethylene, and desorption of ethylene all appear to control the rate of ethylene formation. Although the activation barriers for the addition of hydrogen to acetylene and to vinyl are somewhat similar, the rates for hydrogen addition to acetylene are much higher due to the significantly higher surface coverages of acetylene over vinyl.

4. Conclusion

A first-principles-based kinetic Monte Carlo algorithm was developed and used to simulate the selective hydrogenation of acetylene and ethylene over the Pd(111) surface. The intrinsic kinetic database used in the simulation was determined from DFT calculations. *Through-surface* lateral interactions between adsorbed species were treated using a BOC model, which was regressed against DFT calculations carried out at different coverages, whereas *through-space* interactions were treated using van der Waals interaction term from the MMFF model. The overall hydrogenation activity and selectivity were examined by carrying out simulations at different temperatures and different acetylene and hydrogen partial pressures. The activity and selectivity appear to be controlled by the relative surface bond strengths, as well as by the surface coverages of the intermediates involved in the surface reaction steps. The simulated apparent activation energy for acetylene hydrogenation was found to be 8.0 kcal/mol, in good agreement with experimental result of 9.6 kcal/mol reported by Molero et al. [5]. The simulated reaction orders for acetylene and hydrogen at 300 K were found to be −0.52 and 1.16, respectively. These results are also in very good agreement with experimental values of −0.66 and 1.03 [5]. The selectivity to ethylene formation varies with temperature and partial pressures of acetylene and hydrogen. Ethylene selectivity increases as the temperature and/or the acetylene partial pressure increases. With respect to hydrogen, however, the ethylene selectivity reaches a maximum 300 Torr (over the range of 100–600 Torr) at 300 K. Although acetylene generally dominates the Pd(111) surface, the selectivity to ethylene production is strongly affected by the hydrogen surface coverage. The rate appears to be controlled by the adsorption of hydrogen onto the surface, the hydrogenation of vinyl to ethylene, and the desorption of ethylene.

A comparison of simulations performed with and without lateral interactions indicates that although there is only a small decrease in the apparent activation barrier if one ignores lateral interactions, there are significant changes in the surface coverage. This results in considerable differences in the calculated selectivity and the acetylene and hydrogen reaction orders. The selectivity for acetylene hydrogenation is shown to depend not only on the surface coverage of the reaction intermediates, but also on the local reaction environment surrounding the active intermediates. The reaction rates and selectivity are driven by an optimal amount of surface hydrogen. The selectivity to ethylene is controlled by a complex interplay of both the thermodynamic differences between acetylene and ethylene adsorption, as well as strong kinetic considerations that control the surface coverage and composition. The results indicate that the lateral interactions between coadsorbates are important for simulating the appropriate kinetics, reaction orders with respect to hydrogen and acetylene, and overall selectivity of acetylene to ethylene.

Acknowledgment

The authors kindly acknowledge financial support from the Dow Chemical Company for this work.

Supplementary appendix

The online version of this article contains additional appendix.

Please visit DOI:10.1016/j.jcat.2006.05.009.

References

[1] E.W. Hansen, M. Neurock, Chem. Eng. Sci. 54 (1999) 3411.
[2] E.W. Hansen, M. Neurock, J. Catal. 196 (2000) 241.
[3] E.W. Hansen, M. Neurock, Surf. Sci. 464 (2000) 91.
[4] E.W. Hansen, M. Neurock, J. Phys. Chem. B 105 (2001) 9218.
[5] H. Molero, B.F. Bartlett, W.T. Tysoe, J. Catal. 181 (1999) 49.
[6] H. Arnold, F. Dobert, J. Gaube, in: G. Ertl, H. Knozinger, J. Weitkamp (Eds.), Hydrogenation Reaction in Handbook of Heterogeneous Catalysis, vol. 5, Wiley–VCH, New York, 1997, p. 2165.
[7] M.W. Brown, A. Penlidis, G. Sullivan, Can. J. Chem. Eng. 69 (1991) 152.
[8] C.N. Thanh, B. Didillon, P. Sarrazin, C. Cameron, U.S. Patent (2000).
[9] Y. Jin, A.K. Datye, E. Rightor, R. Gulotty, W. Waterman, M. Smith, M. Holbrook, J. Maj, J. Blackson, J. Catal. 203 (2001) 292.
[10] A. Molnar, A. Sarkany, M. Varga, J. Mol. Catal. A 173 (2001) 185.
[11] T.T.P. Cheung, M.M. Johnson, U.S. Patent 5583274 (1996).
[12] A.N.R. Bos, E.S. Bootsma, F. Foeth, H.W.J. Sleyster, K.R. Westerterp, Chem. Eng. Process. 32 (1993) 53.

[13] G.C. Bond, D.A. Dowden, N. Mackenzie, Trans. Faraday Soc. 54 (1958) 1537.
[14] G.C. Bond, P.B. Wells, J. Catal. 4 (1965) 211.
[15] G.C. Bond, P.B. Wells, J. Catal. 5 (1965) 65.
[16] G.C. Bond, P.B. Wells, J. Catal. 6 (1966) 397.
[17] J. Margitfalvi, L. Guczi, A.H. Weiss, J. Catal. 72 (1981) 185.
[18] J. Horiuti, M. Polanyi, Trans. Faraday Soc. 30 (1934) 1164.
[19] J. Margitfalvi, L. Guczi, A.H. Weiss, React. Kinet. Catal. Lett. 15 (1980) 475.
[20] G.C. Bond, Catalysis by Metals, Academic Press, London, 1962.
[21] W.T. McGown, C. Kemball, D.A. Whan, J. Catal. 51 (1978) 173.
[22] L. Cider, N.H. Schoon, Appl. Catal. 68 (1991) 191.
[23] S. Azad, M. Kaltchev, D. Stacchiola, G. Wu, W.T. Tysoe, J. Phys. Chem. B 104 (2000) 3107.
[24] A. Borodzinski, A. Cybulski, Appl. Catal. A 198 (2000) 51.
[25] A. Borodzinski, A. Golebiowski, Langmuir 13 (1997) 883.
[26] A. Sandell, A. Beutler, A. Jaworowski, M. Wiklund, K. Heister, R. Nyholm, J.N. Anderson, Surf. Sci. 415 (1998) 411.
[27] X.C. Guo, R.J. Madix, J. Catal. 155 (1995) 336.
[28] W.T. Tysoe, R.M. Ormerod, R.M. Lambert, G. Zgrablich, A. Ramirezcuesta, J. Phys. Chem. 97 (1993) 3365.
[29] L.L. Kesmodel, G.D. Waddill, J.A. Gates, Surf. Sci. 138 (1983) 464.
[30] V. Pallassana, M. Neurock, V.S. Lusvardi, J.J. Lerou, D.D. Kragten, R.A. Van Santen, J. Phys. Chem. B 106 (2002) 1656.
[31] P.A. Sheth, M. Neurock, C.M. Smith, J. Phys. Chem. B 107 (2003) 2009.
[32] A.N.R. Bos, K.R. Westerterp, Chem. Eng. Process. 32 (1993) 1.
[33] M. Neurock, D.H. Mei, Top. Catal. 20 (2002) 5.
[34] M. Neurock, E.W. Hansen, Comput. Chem. Eng. 22 (1998) S1045.
[35] D.H. Mei, E.W. Hansen, M. Neurock, J. Phys. Chem. B 107 (2003) 798.
[36] E.W. Hansen, M. Neurock, Surf. Sci. 441 (1999) 410.
[37] D. Duca, P. Baranyai, T. Vidoczy, J. Comput. Chem. 19 (1998) 396.
[38] D. Duca, G. La Manna, M.R. Russo, Phys. Chem. Chem. Phys. 1 (1999) 1375.
[39] D. Duca, L. Botar, T. Vidoczy, J. Catal. 162 (1996) 260.
[40] D. Duca, G. Barone, Z. Varga, Catal. Lett. 72 (2001) 17.
[41] A.S. McLeod, L.F. Gladden, Catal. Lett. 43 (1997) 189.
[42] A.S. McLeod, Catal. Today 53 (1999) 289.
[43] D.H. Mei, E.W. Hansen, M. Neurock, J. Phys. Chem. B 107 (2003) 798.
[44] A. Borodzinski, Catal. Lett. 63 (1999) 35.
[45] S. Asplund, J. Catal. 158 (1996) 267.
[46] W.J. Kim, J.H. Kang, I.Y. Ahn, S.H. Moon, J. Catal. 226 (2004) 226.
[47] T. Mitsui, M.K. Rose, E. Fomin, D.F. Ogletree, M. Salmeron, Nature 422 (2003) 705.
[48] T. Mitsui, M.K. Rose, E. Fomin, D.F. Ogletree, M. Salmeron, Surf. Sci. 540 (2003) 5.
[49] M. Neurock, R.A. Van Santen, J. Phys. Chem. B 104 (2000) 11127.
[50] M. Neurock, in: G.F. Froment, K.C. Waugh (Eds.), Dynamics of Surfaces and Reaction Kinetics in Heterogeneous Catalysis, in: Stud. Surf. Sci. Catal., vol. 109, Elsevier Science, Amsterdam, 1997, p. 3.
[51] G. Kresse, J. Furthmuller, Phys. Rev. B 54 (1996) 11169.
[52] G. Mills, H. Jonsson, G.K. Schenter, Surf. Sci. 324 (1995) 305.
[53] T.A. Halgren, J. Comput. Chem. 17 (1996) 490.
[54] T.A. Halgren, J. Comput. Chem. 17 (1996) 520.
[55] L.D. Kieken, M. Neurock, D.H. Mei, J. Phys. Chem. B 109 (2005) 2234.
[56] J. Rekoske, R. Cortright, S. Goddard, S. Sharma, J. Dumesic, J. Phys. Chem. 96 (1992) 1880.
[57] R. Cortright, S. Goddard, J. Rekoske, J. Dumesic, J. Catal. 127 (1991) 342.
[58] D.H. Mei, Q. Ge, M. Neurock, L. Kieken, J.J. Lerou, Mol. Phys. 102 (2004) 361.
[59] E.W. Hansen, M. Neurock, J. Catal. 196 (2000) 241.
[60] E. Hansen, M. Neurock, J. Phys. Chem. B 105 (2001) 9218.
[61] L.Z. Gva, K.E. Kho, Kinet. Catal. 29 (1988) 331.
[62] Y. Inoue, I. Yasumori, J. Phys. Chem. 75 (1971) 880.
[63] P.S. Cremer, X.C. Su, Y.R. Shen, G.A. Somorjai, Catal. Lett. 40 (1996) 143.
[64] D. Stacchiola, S. Azad, L. Burkholder, W.T. Tysoe, J. Phys. Chem. B 105 (2001) 11233.
[65] T.V.W. Janssens, S. Volkening, T. Zambelli, J. Wintterlin, J. Phys. Chem. B 102 (1998) 6521.
[66] W. Tysoe, G. Nyberg, R. Lambert, Surf. Sci. 135 (1983) 128.
[67] I.M. Abdelrehim, T.E. Caldwell, D.P. Land, J. Phys. Chem. 100 (1996) 10265.
[68] G. Pacchioni, R.M. Lambert, Surf. Sci. 304 (1994) 208.